Synthesis and Reactivity of Rhodium Complex Bearing a PNiP Pincer Ligand

Kouki Fujita, Kazuhiko Semba,*,† and Yoshiaki Nakao*
Department of Material Chemistry, Graduate School of Engineering, Kyoto University, Katsura, Nishikyo-ku, Kyoto, 615-8510, Japan.

ABSTRACT: Rhodium complexes bearing a pincer-type ligand containing nickel were successfully synthesized. Through single-crystal X-ray diffraction analyses and theoretical calculations, the electronic structures of the bimetallic complexes were elucidated. Notably, this represents the inaugural synthesis of a bimetallic complex featuring a distinct nickel–rhodium bond. The reactivity of these synthesized complexes was probed through catalytic arene C–H borylation reactions.

Metalloligands have been found to exhibit properties distinct from conventional ligands based on main group elements, such as strong electron-donicity due to their low electronegativity and unique catalysis facilitated by metal-ligand cooperation.[1] In particular, metalloligands based on transition-metals have received considerable attention due to their unique electronic properties.[2] For example, paddlewheel-type dinuclear RhRh complexes are known to exhibit high catalytic activity in cyclopropanation and C–H insertion reactions through rhodium carbenoids stabilized by a high-energy π* orbital resulting from the interaction of the two rhodium's d-orbitals.[3] The diverse orbital interactions such as σ-, π-, and/or δ-bonding through d-orbitals have been exploited in several dinuclear complexes.[2,4-10] Their unusual redox properties and bimetallic cooperative catalysis are noteworthy.

The concept of metallopincer ligands is often useful for incorporating metalloligands. Because metallopincer ligands can form thermodynamically stable dinuclear complexes by chelating effects, the synthesis of various dinuclear complexes and their catalysis have been reported.[1] For instance, our group reported the synthesis of a rhodium complex bearing a PAlP pincer ligand[11], enabling site-selective C–H functionalization of pyridine[11,12] as well as C–F[13] and C–O[14] activation reactions. Its reactivity arises from low electronegativity and an empty p-orbital of the aluminyl ligand. The former causes high σ-donicity and polarized metal–metal bonds, while the latter provides Lewis acidity. Metallopincer ligands have conventionally been based on main group metals, whereas few examples based on transition-metals, which are anticipated to control the reactivity of coordinating transition-metal center through their diverse orbital interactions and offer robust metal–metal bonds, have been reported.[15] Here we report the synthesis of a PNiP pincer ligand and its corresponding rhodium complexes.

A novel PNNNP ligand **1** was successfully synthesized in 10% yield over 6 steps (see Scheme S1 in the Supporting Information). The reaction of **1** with 1.0 equivalent of $NiCl_2$(dme) (dme: 1,2-dimethoxyethane) in CH_2Cl_2, followed by the addition of 0.50 equivalents of $[RhCl(nbd)]_2$ (nbd: 2,5-norbornadiene), resulting in the formation of rhodium–nickel bimetallic complex **1-NiRh** in 63% yield (Scheme 1). The complex exhibited paramagnetic behavior, and its formation was confirmed by ESI-HRMS. The solid-state structure of **1-NiRh** was elucidated through single-crystal X-ray diffraction analysis (Scheme 1). In **1-NiRh**, nickel adopts a trigonal bipyramidal geometry, while rhodium exhibits a square planar configuration. The measured distance between nickel and rhodium (2.5733(5) Å) closely approximates the sum of their covalent radii (2.66 Å).[16] The formal shortness ratio (FSR), defined as the ratio of the distance between the two metal centers to the sum of their single-bond covalent radii, is 0.97 for **1-NiRh**, suggesting bonding interaction between nickel and rhodium.[17]

Scheme 1. Synthesis of rhodium complex bearing a pincer-type ligand containing nickel 1-NiRh.

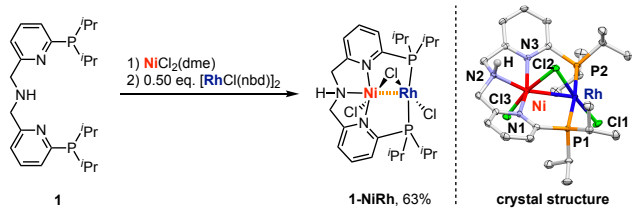

Crystal structures of **1-NiRh** with thermal ellipsoids set at 50% probability; H atoms except for **N2H** were omitted for clarity.

To determine the spin state of **1-NiRh**, geometry optimization and energy calculation were carried out by DFT calculations for three assumed spin states: singlet, triplet, and quintet. Comparing the sum of electronic and thermal free energy for each spin state, the energy for the triplet state was approximately 25~27 kcal/mol lower. Furthermore, comparing the optimized structures to the crystal one, the bond distances around the metals in the triplet state also appeared to be the most reasonable. The calculation results are consistent with **1-NiRh** being paramagnetic. The molecular orbitals depicting the interaction of the d-orbitals of nickel and rhodium are illustrated in Figure 1a. HOMO and HOMO–1 are formed by the antibonding interaction between the d-orbitals of the two metals. As a result of these antibonding interactions, there is

an increase in the energy level of the orbitals. HOMO–9 and HOMO–36 are predominantly localized on nickel, rhodium, chlorines, and **N2**, primarily comprising σ-bonding interactions between nickel and rhodium. To investigate the metal–metal interactions, NBO (Natural Bond Orbital) analysis was conducted for **1-NiRh**. The Wiberg bond index for the nickel–rhodium bond of **1-NiRh** was 0.2567, suggesting the bonding interactions. Moreover, the high spin density of nickel in **1-NiRh** has also been revealed (Table 1). The visualization of molecular orbitals identified that the SOMO of **1-NiRh** was dz^2 and dx^2–y^2 of nickel (Figure 1b). This observation is consistent with the high spin density values associated with the dx^2–y^2 and dz^2 orbitals of the nickel.

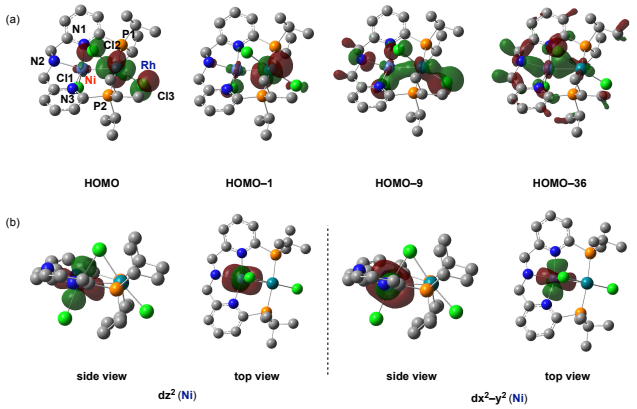

Figure 1. (a) Molecular orbitals depicting the interaction between nickel and rhodium. (b) SOMO of **1-NiRh** (NBO).

Table 1. Spin densities of 1-NiRh.

	Ni	Rh
dxy	–0.00002	0.00206
dxz	0.00412	0.00186
dyz	0.15761	0.10706
dx^2–y^2	0.69583	0.03349
dz^2	0.58659	0.02940

Next, reduction of **1-NiRh** to form a reduced bimetallic complex was investigated. The incorporation of nickel and rhodium to **1** followed by the addition of 2.3 equivalents of KC_8, resulted in the formation of **2-NiRh** in 36% yield (Scheme 2). The complex exhibited diamagnetic behavior, and was characterized by ^{1}H, ^{13}C, and ^{31}P NMR spectroscopies and CSI-HRMS. A signal observed in the ^{1}H NMR spectrum (at –21.72 ppm, dt, J = 27.7, 13.4 Hz P–Rh–*H*) indicated a rhodium hydride. The solid-state structure of **2-NiRh** was also identified through single-crystal X-ray diffraction analysis (Scheme 2). Remarkably, the structure of **2-NiRh** shows dearomatization caused by the loss of the benzylic hydrogens of **1-NiRh**. Additionally, it was observed that one chlorine atom (**Cl3**) was removed from nickel, while another chlorine atom (**Cl2**) was displaced with a hydrogen atom. This intriguing transformation would proceed possibly through two-electron reduction of nickel and oxidative addition of N–H (Scheme 3). Subsequently, reductive elimination of H_2 and isomerization to form enamine was followed by β-hydride elimination, and lastly, hydride migration provided **2-NiRh**.[18] **2-NiRh** was not obtained when **1-NiRh** reacted with 3.0 equivalents of KO^{t}Bu (see the Supporting Information), which supports the notion that two-electron reduction is crucial in this reaction. As evidenced by the flattening of the ligand backbone, the dearomatization process can be driven by the extension of the π-conjugation. Both nickel and rhodium in **2-NiRh** exhibit a square planar configuration, with their distance measured at 2.5279(5) Å. The FSR value of 0.95 for **2-NiRh** implies a single bond between nickel and rhodium. The shorter metal–metal distance observed in **2-NiRh** compared to **1-NiRh** suggests stronger bonding interactions in **2-NiRh**.

Scheme 2. Synthesis of rhodium complex bearing a pincer-type ligand containing nickel 2-NiRh.

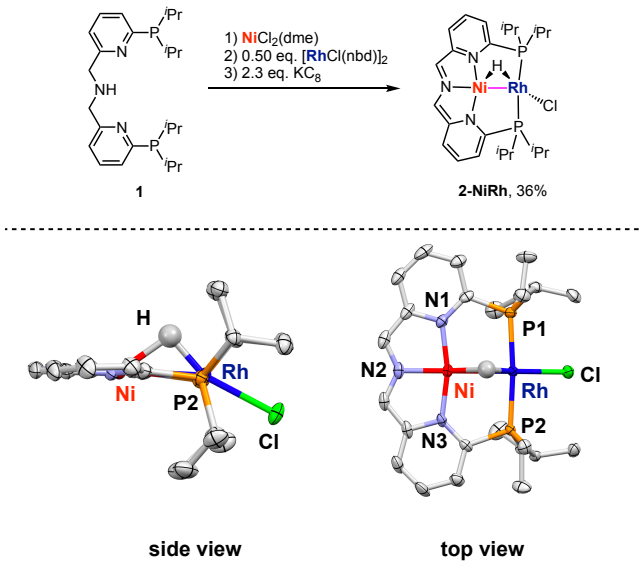

Crystal structures of **2-NiRh** with thermal ellipsoids set at 50% probability; H atoms except for **RhH** were omitted for clarity.

Scheme 3. Mechanism of transformation from 1-NiRh to 2-NiRh.

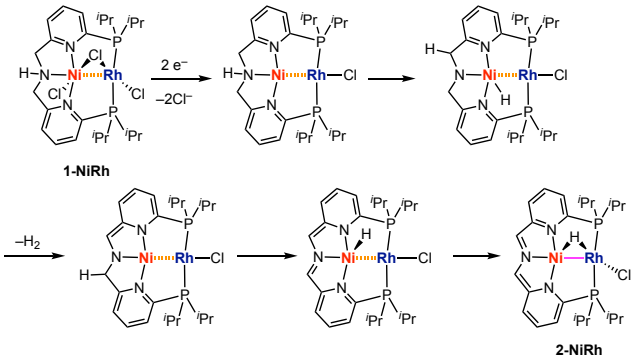

Geometry optimization by DFT calculation for **2-NiRh** was employed to determine the location of the hydrogen atom on rhodium. Two types of structures, with rhodium exhibiting either a square planar or trigonal bipyramidal configuration, were considered. Each of these structures was utilized as the initial configuration for geometry optimization (Figure 2a). As a result, both optimized structures converged to the former. The stretching frequency of the rhodium–hydride bond estimated from the optimized structure was ν(Rh–H) = 1782.3

cm^{-1}. This was experimentally confirmed, with the observed value of ν(Rh–H) = 1863.7 cm^{-1} obtained from infrared spectroscopy, providing strong evidence for a distinct Rh–H bond. Several molecular orbitals exhibiting bonding or antibonding interaction between the metals were found (Figure 2b). Although all orbitals that involve interactions between metals cannot be enumerated because of the complexity induced by participation of the orbitals of the other ligands, it is sufficient to explain the electronic perturbation arising from d-orbital interactions. HOMO comprises dz^2 of rhodium and dxz of nickel, indicating an antibonding interaction. Additionally, HOMO–4 and HOMO–6 also form δ* and π* molecular orbital, respectively. Thus, the energy levels of the rhodium d-orbitals are elevated by those of the nickel ligand. σ-, π-, and δ-Bonding interactions between the metals are found in HOMO–2, –8, –10, –12, –13, and, –32, suggesting the presence of a metal–metal bond. These diverse bonding/antibonding interactions are distinctive of the metalloligands based on transition-metals. NBO analysis was also conducted for **2-NiRh**. The Wiberg bond index for the nickel–rhodium bond was 0.3020, suggesting bonding interactions between the metals. Considering these values in addition to the earlier discussion on bond distances and the molecular orbitals, it can be concluded that **2-NiRh** has a definite nickel–rhodium bond. As far as our search in The Cambridge Crystallographic Data Centre (CCDC) reveals, this is the first instance of a bimetallic complex where nickel and rhodium are bonded.

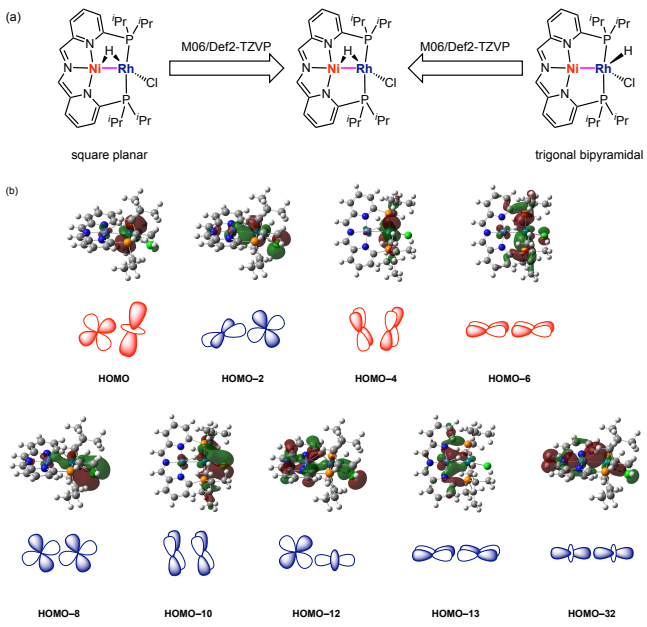

Figure 2. (a) Determination of the location of the hydride via DFT calculations. (b) Characteristic interactions between nickel and rhodium (red: antibonding, blue: bonding).

To investigate the catalytic activity of the synthesized complexes, an arene C–H borylation reaction was attempted.[19] The reaction of benzene (5.6 mmol) with B_2pin_2 (0.10 mmol, B_2pin_2: bis(pinacolato)diboron) in the presence of **2-NiRh** (5 mol% of B_2pin_2) and KO^{t}Bu (6 mol%) in neat conditions at 120 °C for 30 h afforded PhBpin in 69% yield based on B_2pin_2 (Table 2, entry 1). The reactivity of **2-NiRh** deteriorated without the addition of KO^{t}Bu (entry 2). The base likely acts as an activator by facilitating the reductive elimination of HCl atoms from the rhodium in **2-NiRh** to form an active catalyst.[20] **1-NiRh** exhibited lower yields than **2-NiRh** (entries 3 and 4). Although the complexes have similar structures, it is remarkable that the slight differences in the interaction of the metals affect the catalyst reactivity. PNNNP ligand **1** with $NiCl_2$(dme) did not show any catalytic activity (entries 5 and 6), whereas **1** with $[RhCl(nbd)]_2$ resulted in the formation of PhB(pin) in moderate yield (entries 7 and 8). Based on these results, it is presumed that this reaction takes place at the rhodium center. The synthesized complexes, especially **2-NiRh,** exhibited superior catalytic activity than the corresponding mononuclear complexes. The tuning of the electronic state, as seen in the conversion from **1-NiRh** to **2-NiRh**, led to a dramatic change in reactivity.

Table 2. Catalytic C–H borylation of benzene with various catalysts.

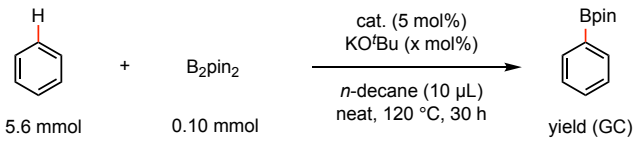

entry	cat.	KO^{t}Bu (x mol%)	conv. (%) (B_2pin_2)	yield (%)
1	**2-NiRh**	6	100	69
2	**2-NiRh**	0	40	7
3	**1-NiRh**	6	22	2
4	**1-NiRh**	0	8	n.d.
5[a]	**1**+$NiCl_2$(dme)	6	27	n.d.
6[a]	**1**+$NiCl_2$(dme)	0	0	n.d.
7[b]	**1**+$[RhCl(nbd)]_2$	6	90	32
8[b]	**1**+$[RhCl(nbd)]_2$	0	61	17

[a] **1** (6 mol%) and $NiCl_2$(dme) (5 mol%) were used. [b] **1** (6 mol%) and $[RhCl(nbd)]_2$ (5 mol%/Rh) were used.

In conclusion, rhodium complexes with nickel-based metallopincer-type ligands have been successfully synthesized and characterized. Theoretical calculations have highlighted the electronic perturbation effect of the nickel ligand on the coordinating rhodium center through various orbital interactions derived from their d-orbitals. Additionally, their potentials as catalysts for C–H functionalization were evaluated through arene C–H borylation reactions. Further explorations in harnessing the complexes for valuable catalytic reactions are in progress.

ASSOCIATED CONTENT

Supporting Information

The Supporting Information is available free of charge on the ACS Publications website.
Experimental procedures, calculation results, crystallographic data, and characterization of compounds (PDF)

AUTHOR INFORMATION

Corresponding Authors

Kazuhiko Semba – Department of Material Chemistry, Graduate School of Engineering, Kyoto University, Katsura, Nishikyo-ku,

Kyoto, 615-8510, Japan; orcid.org/0000-0001-7903-4091; Email: semba.kazuhiko.5n@kyoto-u.ac.jp

Yoshiaki Nakao – Department of Material Chemistry, Graduate School of Engineering, Kyoto University, Katsura, Nishikyo-ku, Kyoto, 615-8510, Japan; orcid.org/0000-0003-4864-3761; Email: nakao.yoshiaki.8n@kyoto-u.ac.jp

Author

Kouki Fujita – Department of Material Chemistry, Graduate School of Engineering, Kyoto University, Katsura, Nishikyo-ku, Kyoto, 615-8510, Japan

Present Addresses

† Department of Energy and Hydrocarbon Chemistry, Graduate School of Engineering, Kyoto University, Katsura, Nishikyo-ku, Kyoto, 615-8510 Japan

Author Contributions

The manuscript was written through contributions of all authors.

Notes

The authors declare no competing financial interest.

ACKNOWLEDGMENT

This work was financially supported by JSPS KAKENHI [Grants Numbers JP20H00376 (Y.N.), JP24H00456 (Y.N.), JP22K19026 (K.S.), and JP24K01483 (K.S.)].

REFERENCES

(1)(a) Hara, N.; Semba, K.; Nakao, Y. X-Type Aluminyl Ligands for Transition-Metal Catalysis. *ACS Catal.* **2022**, *12*, 1626–1638. (b) Yamashita, M. The Organometallic Chemistry of Boron-Containing Pincer Ligands Based on Diazaboroles and Carboranes. *Bull. Chem. Soc. Jpn.* **2016**, *89*, 269–281. (c) Takaya, J. Catalysis using transition metal complexes featuring main group metal and metalloid compounds as supporting ligands. *Chem. Sci.* **2021**, *12*, 1964–1981. (d) Komuro, T.; Nakajima, Y.; Takaya, J.; Hashimoto, H. Recent progress in transition metal complexes supported by multidentate ligands featuring group 13 and 14 elements as coordinating atoms. *Coord. Chem. Rev.* **2022**, *473*, 214837.

(2)(a) Powers, I. G.; Uyeda, C. Metal–Metal Bonds in Catalysis. *ACS Catal.* **2017**, *7*, 936–958. (b) Cooper, B. G.; Napoline, J. W.; Thomas, C. M. Catalytic Applications of Early/Late Heterobimetallic Complexes. *Catal. Rev. Sci. Eng.* **2012**, *54*, 1–40.

(3)(a) Hubert, A. J.; Noels, A. F.; Anciaux, A. J.; Teyssié, P. Rhodium(II) Carboxylates: Novel Highly Efficient Catalysts for the Cyclopropanation of Alkenes with Alkyl Diazoacetates. *Synthesis* **1976**, 600–602. (b) Demonceau, A.; Noels, A. F.; Hubert, A. J.; Teyssié, P. Transition-metal-catalysed reactions of diazoesters. Insertion into C–H bonds of paraffins by carbenoids. *J. Chem. Soc., Chem. Commun.* **1981**, 688–689. (c) Berry, J. F. The role of three-center/four-electron bonds in superelectrophilic dirhodium carbene and nitrene catalytic intermediates. *Dalton Trans.* **2012**, *41*, 700–713. (d) Pirrung, M. C.; Liu, H.; Morehead, A. T. Rhodium Chemzymes: Michaelis−Menten Kinetics in Dirhodium(II) Carboxylate-Catalyzed Carbenoid Reactions. *J. Am. Chem. Soc.* **2002**, *124*, 1014–1023. (e) Gillingham, D.; Fei, N. Catalytic X–H insertion reactions based on carbenoids. *Chem. Soc. Rev.* **2013**, *42*, 4918–4931. (f) Davies, H. M. L.; Manning, J. R. Catalytic C–H insertion reactions based on carbenoids. *Nature* **2008**, *451*, 417–424.

(4)(a) Wang, Q.; Brooks, S. H.; Liu, T.; Tomson, N. C. Tuning metal–metal interactions for cooperative small molecule activation. *Chem. Commun.* **2021**, *57*, 2839–2853. (b) Deolka, S.; Rivada-Wheelaghan, O.; Aristizábal, S. L.; Fayzullin, R. R.; Pal, S.; Nozaki, K.; Khaskin, E.; Khusnutdinova, J. R. Metal–metal cooperative bond activation by heterobimetallic alkyl, aryl, and acetylide Pt^{II}/Cu^{I} complexes. *Chem. Sci.* **2020**, *11*, 5494–5502. (c) Chipman, J. A.; Berry, J. F. Paramagnetic Metal–Metal Bonded Heterometallic Complexes. *Chem. Rev.* **2020**, *120*, 2409–2447.

(5)(a) Nishibayashi, Y.; Wakiji, I.; Hidai, M. Novel Propargylic Substitution Reactions Catalyzed by Thiolate-Bridged Diruthenium Complexes via Allenylidene Intermediates. *J. Am. Chem. Soc.* **2000**, *122*, 11019–11020. (b) Ammal, S. C.; Yoshikai, N.; Inada, Y.; Nishibayashi, Y.; Nakamura, E. Synergistic Dimetallic Effects in Propargylic Substitution Reaction Catalyzed by Thiolate-Bridged Diruthenium Complex. *J. Am. Chem. Soc.* **2005**, *127*, 9428–9438.

(6)(a) Zhou, Y.-Y.; Hartline, D. R.; Steiman, T. J.; Fanwick, P. E.; Uyeda, C. Dinuclear Nickel Complexes in Five States of Oxidation Using a Redox-Active Ligand. *Inorg. Chem.* **2014**, *53*, 11770–11777. (b) Zhou, Y.-Y.; Uyeda, C. Catalytic reductive [4 + 1]-cycloadditions of vinylidenes and dienes. *Science* **2019**, *363*, 857–862. (c) Hartline, D. R.; Zeller, M.; Uyeda, C. Well-Defined Models for the Elusive Dinuclear Intermediates of the Pauson–Khand Reaction. *Angew. Chem. Int. Ed.* **2016**, *55*, 6084–6087. (d) Hartline, D. R.; Zeller, M.; Uyeda, C. Catalytic Carbonylative Rearrangement of Norbornadiene via Dinuclear Carbon–Carbon Oxidative Addition. *J. Am. Chem. Soc.* **2017**, *139*, 13672–13675. (e) Steiman, T. J.; Uyeda, C. Reversible Substrate Activation and Catalysis at an Intact Metal–Metal Bond Using a Redox-Active Supporting Ligand. *J. Am. Chem. Soc*. **2015**, *137*, 6104–6110.

(7)(a) Greenwood, B. P.; Forman, S. I.; Rowe, G. T.; Chen, C.-H.; Foxman, B. M.; Thomas, C. M. Multielectron Redox Activity Facilitated by Metal−Metal Interactions in Early/Late Heterobimetallics: Co/Zr Complexes Supported by Phosphinoamide Ligands. *Inorg. Chem.* **2009**, *48*, 6251–6260. (b) Greenwood, B. P.; Rowe, G. T.; Chen, C.-H.; Foxman, B. M.; Thomas, C. M. Metal−Metal Multiple Bonds in Early/Late Heterobimetallics Support Unusual Trigonal Monopyramidal Geometries at both Zr and Co. *J. Am. Chem. Soc.* **2009**, *132*, 44–45. (c) Zhou, W.; Marquard, S. L.; Bezpalko, M. W.; Foxman, B. M.; Thomas, C. M. Catalytic Hydrosilylation of Ketones Using a Co/Zr Heterobimetallic Complex: Evidence for an Unusual Mechanism Involving Ketyl Radicals. *Organometallics* **2013**, *32*, 1766–1772.

(8)(a) Nagashima, H.; Sue, T.; Oda, T.; Kanemitsu, A.; Matsumoto, T.; Motoyama, Y.; Sunada, Y. Dynamic Titanium Phosphinoamides as Unique Bidentate Phosphorus Ligands for Platinum. *Organometallics* **2006**, *25*, 1987–1994. (b) Sunada, Y.; Sue, T.; Matsumoto, T.; Nagashima, H. Titanium(IV) phosphinoamide as a unique bidentate ligand for late transition metals II: Ti–Ru heterobimetallics bearing a bridging chlorine atom. *J. Organomet. Chem.* **2006**, *691*, 3176–3182. (c) Sue, T.; Sunada, Y.; Nagashima, H. Zirconium(IV) Tris(Phosphinoamide) Complexes as a Tripodal-Type Metalloligand: A Route to Zr–M (M = Cu, Mo, Pt) Heterodimetallic Complexes. *Eur. J. Inorg. Chem.* **2007**, 2897–2908. (d) Tsutsumi, H.; Sunada, Y.; Shiota, Y.; Yoshizawa, K.; Nagashima, H. Nickel(II), Palladium(II), and Platinum(II) η^3-Allyl Complexes Bearing a Bidentate Titanium(IV) Phosphinoamide Ligand: A Ti←M_2 Dative Bond Enhances the Electrophilicity of the π-Allyl Moiety. *Organometallics* **2009**, *28*, 1988–1991.

(9)(a) Jacobsen, E. N.; Goldberg, K. I.; Bergman, R. G. Rapid, Reversible Intramolecular C–H Oxidative Addition and Hydrogen Exchange in a Heterodinuclear "Early–Late" Transition-Metal Complex. *J. Am. Chem. Soc.* **1988**, *110*, 3706–3707. (b) Goldberg, K. I.; Bergman, R. G. Synthesis and Physical Properties of a Dinuclear Tantalum–Cobalt Radical with Spin Localized at One Metal Center. *J. Am. Chem. Soc.* **1988**, *110*, 4853–4855. (c) Hostetler, M. J.; Bergman, R. G. Synthesis and Reactivity of $Cp_2Ta(CH_2)_2Ir(CO)_2$: An Early–Late Heterobimetallic Complex That Catalytically Hydrogenates, Isomerizes and Hydrosilates Alkenes. *J. Am. Chem. Soc.* **1990**, *112*, 8621–8623.

(10)(a) Khand, I. U.; Knox, G. R.; Pauson, P. L.; Watts, W. E. A Cobalt Induced Cleavage Reaction and a New Series of Arenecobalt Carbonyl Complexes. *J. Chem. Soc. D.* **1971**, 36a–36a. (b) Yamanaka, M.; Nakamura, E. Density Functional Studies on the Pauson−Khand Reaction. *J. Am. Chem. Soc.* **2001**, *123*, 1703–1708. (c) Magnus, P.; Principe, L. M. Origins of 1,2- and 1,3-stereoselectivity in dicobaltoctacarbonyl alkene-alkyne cyclizations for the synthesis of

substituted bicyclo[3.3.0]octenones. *Tetrahedron Lett.* **1985**, *26*, 4851–4854.

(11) Hara, N.; Saito, T.; Semba, K.; Kuriakose, N.; Zheng, H.; Sakaki, S.; Nakao, Y. Rhodium Complexes Bearing PAlP Pincer Ligands. *J. Am. Chem. Soc.* **2018**, *140*, 7070–7073.

(12)(a) Hara, N.; Uemura, N.; Nakao, Y. C2-Selective silylation of pyridines by a rhodium–aluminum complex. *Chem. Commun.* **2021**, *57*, 5957–5960. (b) Hara, N.; Aso, K.; Li, Q.-Z.; Sakaki, S.; Nakao, Y. C2-Selective alkylation of pyridines by rhodium–aluminum complexes. *Tetrahedron* **2021**, *95*, 132339.

(13)(a) Fujii, I.; Semba, K.; Li, Q.-Z.; Sakaki, S.; Nakao, Y. Magnesiation of Aryl Fluorides Catalyzed by a Rhodium–Aluminum Complex. *J. Am. Chem. Soc.* **2020**, *142*, 11647–11652. (b) Nakao, Y.; Fujii, I.; Higo, R.; Semba, K. Magnesiation of Alkyl Fluorides Catalyzed by Rhodium–Aluminum Bimetallic Complexes. *Synlett* **2024**, *35*, 455–458.

(14) Seki, R.; Hara, N.; Saito, T.; Nakao, Y. Selective C–O Bond Reduction and Borylation of Aryl Ethers Catalyzed by a Rhodium–Aluminum Heterobimetallic Complex. *J. Am. Chem. Soc.* **2021**, *143*, 6388–6394.

(15)(a) Tanaka, K.; Iwasawa, N.; Takaya, J. Syntheses and Reactivities of Rhodium-Palladium Bimetallic Complexes. In *The 103rd CSJ Annual Meeting*, Japan, **2023**, K502-3am-11. (b) Yang, S.; Morita, Y.; Nakamura, Y.; Iwasawa, N.; Takaya, J. Tuning Photoredox Catalysis of Ruthenium with Palladium: Synthesis of Heterobimetallic Ru–Pd Complexes That Enable Efficient Photochemical Reduction of CO_2. *J. Am. Chem. Soc.* **2024**, https://doi.org/10.1021/jacs.3c14338.

(16) Cordero, B.; Gómez, V.; Platero-Prats, A. E.; Revés, M.; Echeverría, J.; Cremades, E.; Barragán, F.; Alvarez, S. Covalent radii revisited. *Dalton Trans.* **2008**, 2832–2838.

(17) Cotton, F. A.; Walton, R. A.; *Multiple Bonds between Metal Atoms*, Wiley, **1982**.

(18)(a) Vogt, M.; Langer, R. The Pincer Platform Beyond Classical Coordination Patterns. *Eur. J. Inorg. Chem.* **2020**, 3885–3898. (b) Oren, D.; Diskin-Posner, Y.; Avram, L.; Feller, M.; Milstein, D. Metal–Ligand Cooperation as Key in Formation of Dearomatized Ni^{II}–H Pincer Complexes and in Their Reactivity toward CO and CO_2. *Organometallics* **2018**, *37*, 2217–2221.

(19) (a) Ishiyama, T.; Takagi, J.; Ishida, K.; Miyaura, N.; Anastasi, N. R.; Hartwig, J. F. Mild Iridium-Catalyzed Borylation of Arenes. High Turnover Numbers, Room Temperature Reactions, and Isolation of a Potential Intermediate. *J. Am. Chem. Soc.* **2002**, *124*, 390–391. (b) Cho, J.-Y.; Tse, M. K.; Holmes, D.; Maleczka, R. E., Jr.; Smith, M. R., III. Remarkably Selective Iridium Catalysts for the Elaboration of Aromatic C-H Bonds. *Science* **2002**, *295*, 305–308. (c) Lee, C.-I.; Hirscher, N. A.; Zhou, J.; Bhuvanesh, N.; Ozerov, O. V. Adaptability of the SiNN Pincer Ligand in Iridium and Rhodium Complexes Relevant to Borylation Catalysis. *Organometallics* **2015**, *34*, 3099–3102. (d) Komuro, T.; Mochizuki, D.; Hashimoto, H.; Tobita, H. Iridium and rhodium complexes bearing a silyl-bipyridine pincer ligand: synthesis, structures and catalytic activity for C–H borylation of arenes. *Dalton Trans.* **2022**, *51*, 9983–9987. (e) Fang, H.; Choe, Y.; Li, Y.; Shimada, S. Synthesis, Structure, and Reactivity of Hydridoiridium Complexes Bearing a Pincer-Type PSiP Ligand. *Chem. Asian. J.* **2011**, *6*, 2512–2521. (f) Hung, M.-U.; Press, L. P.; Bhuvanesh, N.; Ozerov, O. V. Examination of a Series of Ir and Rh PXL Pincer Complexes as (Pre)Catalysts for Aromatic C–H Borylation. *Organometallics* **2021**, *40*, 1004–1013.

(20) Segawa, Y.; Yamashita, M.; Nozaki, K. Syntheses of PBP Pincer Iridium Complexes: A Supporting Boryl Ligand. *J. Am. Chem. Soc.* **2009**, *131*, 9201–9203.

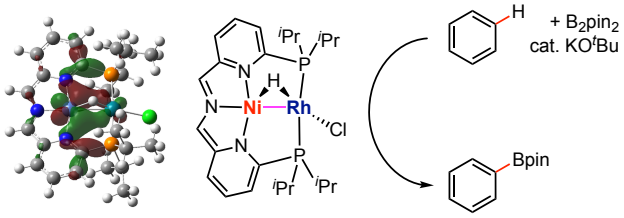

✔ *diverse orbital interactions* ✔ *Ni–Rh bond* ✔ *catalytic C–H borylation*